# Prescribed-Time Attitude Control of Combined Spacecraft Based on Disturbance Observer

*ZHANG Hao*[1], *MA Songjing*[1], *HUA Bing*[1], *LU Zhenkun*[2*], *WU Yunhua*[1*]

1. College of Astronautics, Nanjing University of Aeronautics and Astronautics, Nanjing 210016, P. R. China;
2. School of Robot Engineering, Wenzhou University of Technology, Wenzhou 325000, P. R. China

(Received 6 August 2025; revised 22 September 2025; accepted 30 December 2025)

**Abstract:** In on-orbit servicing missions, the servicing spacecraft typically docks with the target spacecraft to form a combined spacecraft to carry out subsequent tasks, and the cooperative attitude control between the two spacecraft is one of the challenging techniques. To address the issues of inertia uncertainty, communication delays, and external disturbances in combined spacecraft attitude control, a prescribed-time attitude cooperative control method based on disturbance observer is proposed. Firstly, a distributed control model for combined spacecraft is established, and a prescribed performance function with directly adjustable convergence time is designed to characterize both the transient and steady-state behaviors of the system. Secondly, integrating the backstepping method, an attitude controller based on prescribed-time performance is developed to achieve fast and accurate attitude maneuvering of the combined spacecraft. Thirdly, a disturbance observer is introduced to estimate the composite disturbance caused by inertia uncertainty and external perturbations. Meanwhile, based on consensus theory, an attitude cooperative controller is designed to compensate for the control torque mismatch caused by communication delays. The system's stability is then proved using Lyapunov method. Finally, numerical simulations demonstrate that the proposed controller achieves accurate cooperative attitude control of combined spacecraft within the prescribed time under the above disturbances.

**Key words:** combined spacecraft; attitude maneuver; prescribed-time control; disturbance observer; robust cooperative control

**CLC number:** TN925 **Document code:** A **Article ID:** 1005-1120(2026)04-0560-15

## 0 Introduction

In recent years, large-scale constellations represented by "Starlink" have launched numerous satellites to compete for dominance in space-based information[1], leading increasing demand for on-orbit servicing of failed spacecraft[2]. Moreover, with the increasing complexity of space missions[3], single spacecraft can no longer meet operation demands. Combined spacecraft systems have emerged as a significant development trend. Typically composed of multiple spacecraft modules, such systems enhance the scalability and reconfigurability, making them suitable for completing complex on-orbit space missions[4]. The combined spacecraft faces significant technical challenges in achieving stable and precise attitude control after on-orbit assembly or docking[5]. Firstly, factors such as the docking process of spacecraft formations, the fuel consumption and the payload movement all contribute to the uncertainty of the spacecraft's moment of inertia[6]. On the other hand, communication delays among modules can induce dynamic coupling effects between spacecraft, leading to reduced attitude control accuracy. As a result, control strategies for single spacecraft are not directly applicable[7]. Moreover, although numerous methods for spacecraft attitude control have been developed, practical engineering missions

*Corresponding authors, E-mail addresses: yunhuawu@nuaa.edu.cn, luzhk123@163.com.

**How to cite this article**: ZHANG Hao, MA Songjing, HUA Bing, et al. Prescribed-time attitude control of combined spacecraft based on disturbance observer[J]. Transactions of Nanjing University of Aeronautics and Astronautics, 2026, 43(4): 560-574.

http://dx.doi.org/10.16356/j.1005-1120.2026.04.006

often require precise control of state performance within desired time. Therefore, it is of great theoretical and practical significance to design a robust cooperative attitude controller with prescribed-time performance for combined spacecraft.

In recent years, extensive researches have been conducted on attitude control of combined spacecraft. Due to fuel consumption and payload movement, the moment of inertia of spacecraft is often uncertain. To address this issue, Huang et al.[8] introduced adaptive terms to compensate for system uncertainties and designed an adaptive backstepping controller to achieve attitude control of tethered combined spacecraft. Wang et al.[9-10] addressed the vibration suppression problem of flexible spacecraft by employing an extended disturbance observer and a dynamic filter to actively estimate and compensate for nonlinear flexible disturbances, thereby improving attitude control accuracy. Zhang et al.[11-12] proposed a tanh-type self-learning control method with variable learning strength, which can achieve the desired control accuracy without the need for an accurate spacecraft dynamic model. Moreover, implementing cooperative control of combined spacecraft requires each sub-spacecraft to obtain attitude information from neighboring spacecraft to determine its own control torque. However, communication delays during information transmission cause difference in the received attitude data[13]. As a key to effective coordination in multi-agent systems[14], distributed cooperative control has attracted widespread attention. Han et al.[15] proposed a backstepping-based cooperative control algorithm for spacecraft formation, enabling multiple spacecraft to track the attitude of the main spacecraft. Liu et al.[16] introduced a queue-based distributed state observer for multi-agent systems with data packet loss and communication delays, and designed a corresponding distributed output feedback control algorithm.

It is worth noting that above methods mainly focused on the steady-state performance of the system. For certain space docking missions, transient performance indicators such as overshoot and convergence time must also be emphasized. To this end, prescribed performance control, which allows a priori specification of both transient and steady-state behavior, has achieved significant progress in spacecraft attitude control since it was proposed by Bechlioulis et al.[17] in 2008. Although traditional exponential prescribed performance functions ensure convergence of the controlled system, the state theoretically reaches the prescribed steady-state performance in infinite time. To accelerate system convergence, Li et al.[18] defined the performance envelope using a prescribed performance function and designed a terminal sliding mode controller to achieve finite-time prescribed performance control. Similar studies on finite-time prescribed performance control can be found in Refs.[19-21]. However, both the sliding surface and controller design require fractional-order of system states, leading to high design complexity. To address this, Hao et al.[22] and Gao et al.[23] conducted prescribed-time control studies based on the backstepping method for attitude control of a single rigid spacecraft. Nonetheless, few studies have focused on prescribed-time cooperative attitude control of combined spacecraft, especially under inertia uncertainty and time-varying communication delays.

Based on the above analysis, this paper investigates prescribed-time cooperative attitude control of combined spacecraft, considering inertia uncertainty, communication delays and external disturbances. Based on prescribed performance control, disturbance observer and consensus theory, a distributed control model for combined spacecraft is built and a robust cooperative control method with prescribed-time convergence is proposed. Firstly, a prescribed performance function that directly sets the convergence time is proposed. Secondly, a barrier-free error transformation function is introduced to remove constraints, providing greater flexibility and robustness in controller design. Exploiting the fast initial and slow terminal response of backstepping, an attitude controller with prescribed-time performance is designed to achieve fast and accurate attitude maneuvers of combined spacecraft. Thirdly, an adaptive disturbance observer is designed to estimate the combined disturbance from inertia uncertainty and external disturbances, enhancing the controller's robustness. Meanwhile, based on consensus theory, a cooperative attitude controller is introduced to compensate for attitude information mismatch caused by communication delays. Finally, numerical simulations verify the effectiveness of the proposed controller, showing that it achieves fast and accurate cooperative attitude control of combined spacecraft within the prescribed time under various external disturbances.

# 1 Modeling and Problem Formulation

## 1.1 Attitude dynamics and kinematics model

The schematic diagram of the combined spacecraft studied in this paper is shown in Fig.1. It is assumed that after the mission spacecraft and the target spacecraft have completed docking, the interface is locked and the configuration remains fixed, allowing the combined system to be modeled as a single rigid body. Each individual spacecraft is equipped with its own sensors, controllers and actuators, and the two controllers coordinate the attitude control of the combined system via wireless communication. Based on the structure of the combined spacecraft, the following coordinate frames are defined: The inertial frame $\mathcal{F}_\mathrm{I}$, the body frame of the combined spacecraft $\mathcal{F}_\mathrm{b}$; and the body frames of the individual spacecraft $\mathcal{F}_{\mathrm{b},k}$.

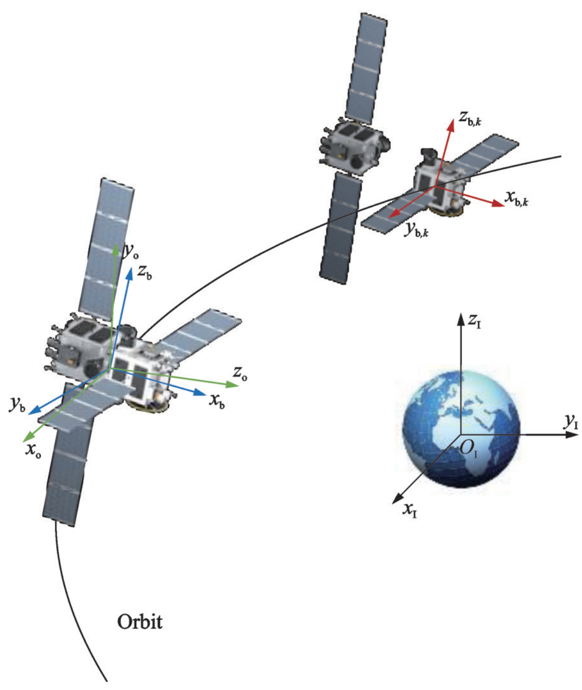


Fig.1 Schematic diagram of the combined spacecraft

The attitude is described via quaternions $\boldsymbol{Q}$ as

$$\boldsymbol{Q}=\begin{bmatrix} q_0 & \boldsymbol{q}^\mathrm{T} \end{bmatrix}^\mathrm{T} \tag{1}$$

The kinematic and dynamic equations[24] of the combined spacecraft are described as

$$\begin{cases} \dot{\boldsymbol{Q}}=\dfrac{1}{2}G(\boldsymbol{Q})\boldsymbol{\omega}=\dfrac{1}{2}\begin{bmatrix} -\boldsymbol{q}^\mathrm{T} \\ q_0\boldsymbol{E}_3+\boldsymbol{q}^\times \end{bmatrix}\boldsymbol{\omega} \\ \boldsymbol{J}\dot{\boldsymbol{\omega}}=-\boldsymbol{\omega}^\times\boldsymbol{J}\boldsymbol{\omega}+\boldsymbol{u}+\boldsymbol{d} \end{cases} \tag{2}$$

where $\boldsymbol{J}=\boldsymbol{J}_0+\Delta\boldsymbol{J}$, $\boldsymbol{J}_0\in\mathbf{R}^{3\times3}$ and $\Delta\boldsymbol{J}\in\mathbf{R}^{3\times3}$ denote the nominal inertia matrix and its uncertainties, respectively. The symbol $\times$ represents the cross-product matrix operator. $\boldsymbol{E}_3$ is the identity matrix, $\boldsymbol{\omega}\in\mathbf{R}^3$ the angular velocity relative to the inertial frame, and $\boldsymbol{d}\in\mathbf{R}^3$ the external disturbance torque. $\boldsymbol{\tau}_k$ is the control torque provided by the individual spacecraft and it is applied to the combined spacecraft, given by

$$\boldsymbol{u}=\sum_{k=1}^{n}\boldsymbol{R}_k^\mathrm{b}\boldsymbol{\tau}_k \tag{3}$$

where $\boldsymbol{R}_k^\mathrm{b}\in\mathbf{R}^3$ is the transformation matrix from the $\mathcal{F}_{\mathrm{b},k}$ to the $\mathcal{F}_\mathrm{b}$.

## 1.2 Error dynamic and kinematic equations

The spacecraft attitude control process can be described as follows: Given a desired attitude $\boldsymbol{Q}_\mathrm{d}$ and desired angular velocity $\boldsymbol{\omega}_\mathrm{d}$, the error quaternion $\boldsymbol{Q}_\mathrm{e}$ and error angular velocity $\boldsymbol{\omega}_\mathrm{e}$ are computed based on the current attitude information. A controller is then designed to steer the spacecraft from its current attitude to the target attitude under external disturbances. Let $\boldsymbol{Q}_\mathrm{d}^*$ be the conjugate quaternion of $\boldsymbol{Q}_\mathrm{d}$, then

$$\begin{cases} \boldsymbol{Q}_\mathrm{e}=\boldsymbol{Q}_\mathrm{d}^*\otimes\boldsymbol{Q} \\ \boldsymbol{\omega}_\mathrm{e}=\boldsymbol{\omega}-\boldsymbol{R}_\mathrm{e}\boldsymbol{\omega}_\mathrm{d} \end{cases} \tag{4}$$

where $\otimes$ denotes quaternion multiplication. $\boldsymbol{R}_\mathrm{e}\in\mathbf{R}^{3\times3}$ is the rotation matrix from the desired attitude frame $\mathcal{F}_\mathrm{d}$ to the $\mathcal{F}_\mathrm{b}$, and can be expressed as

$$\boldsymbol{R}_\mathrm{e}=(q_{\mathrm{e}0}^2-\boldsymbol{q}_\mathrm{e}^\mathrm{T}\boldsymbol{q}_\mathrm{e})\boldsymbol{E}_3+2\boldsymbol{q}_\mathrm{e}\boldsymbol{q}_\mathrm{e}^\mathrm{T}-2q_{\mathrm{e}0}\boldsymbol{q}_\mathrm{e}^\times \tag{5}$$

Substituting Eq.(4) into Eq.(2), the error kinematic and dynamic equations are obtained as

$$\begin{cases} \dot{\boldsymbol{Q}}_\mathrm{e}=\dfrac{1}{2}G(\boldsymbol{Q}_\mathrm{e})\boldsymbol{\omega}_\mathrm{e}=\dfrac{1}{2}\begin{bmatrix} -\boldsymbol{q}_\mathrm{e}^\mathrm{T} \\ q_{\mathrm{e}0}\boldsymbol{E}_3+\boldsymbol{q}_\mathrm{e}^\times \end{bmatrix}\boldsymbol{\omega}_\mathrm{e} \\ \boldsymbol{J}\dot{\boldsymbol{\omega}}_\mathrm{e}=-\boldsymbol{\omega}^\times\boldsymbol{J}\boldsymbol{\omega}+\boldsymbol{J}\boldsymbol{\omega}_\mathrm{e}^\times\boldsymbol{R}_\mathrm{e}\boldsymbol{\omega}_\mathrm{d}-\boldsymbol{J}\boldsymbol{R}_\mathrm{e}\dot{\boldsymbol{\omega}}_\mathrm{d}+\boldsymbol{u}+\boldsymbol{d} \end{cases} \tag{6}$$

## 2 Attitude Controller Design for the Combined Spacecraft

The control process is described as follows: For the combined spacecraft under inertia uncertainty, attitude error, communication delay and external disturbance, a robust cooperative controller based on prescribed performance is designed. It is worth noting that controller 1 and controller 2 are identical in both structure and parameters. The control architecture is shown in Fig.2.

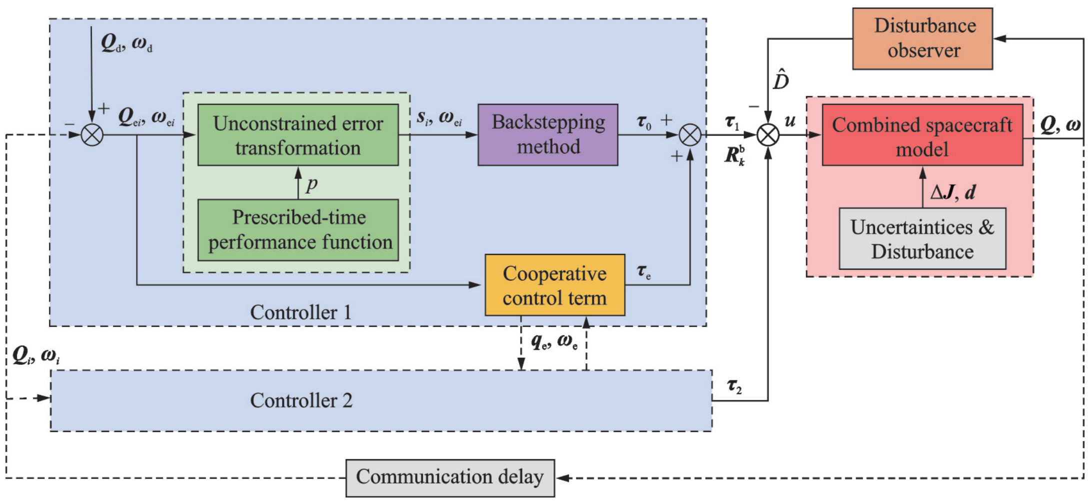


Fig.2 Block diagram of the attitude control system

### 2.1 Design of prescribed-time performance function

According to the definition of prescribed performance bounds in Ref.[25], the attitude error $\boldsymbol{q}_e$ is constrained within the following performance envelope

$$-\underline{\delta}_i p_i(t) < q_{ei}(t) < \bar{\delta}_i p_i(t) \tag{7}$$

where $\underline{\delta}_i, \bar{\delta}_i \in (0,1]$, $i=1,2,3$ denotes the overshoot suppression parameter for tuning overshoot and undershoot, and $p_i(t)>0$ the strictly decreasing performance function. In addition, define the normalized error $\vartheta_i(t)=q_{ei}(t)/p_i(t)\in(-\underline{\delta}_i, \bar{\delta}_i)$.

To ensure the system states enter the stability region within a prescribed time, where the convergence time is directly set by the user, and to differ from the traditional exponential performance function, a faster-converging prescribed-time performance function (PPF) is adopted, and defined as follows

$$p_i(t)=\begin{cases}(p_{i,0}-p_{i,\infty})(1-t/T_d)^{\frac{1}{1-k}}+p_{i,\infty} & 0\leqslant t<T_d \\ p_{i,\infty} & t\geqslant T_d\end{cases} \tag{8}$$

where $T_d$ is the prescribed convergence time, $k$ a positive constant and $k\in(0,1)$, $p_{i,0}$ the initial value of the performance function $p_i(t)$, satisfying $p_{i,0}>|q_{ei}(0)|$ and $p_{i,\infty}$ the final value of $p_i(t)$.

The introduction of performance constraints imposes additional nonlinear restrictions on the system, increasing the complexity of the corresponding controller design. To facilitate controller design, the constrained state variables are transformed into unconstrained ones by converting the constrained attitude error into an equivalent unconstrained state, satisfying $q_{ei}(t)=h(s_i(t))p_i(t)$. Different from the traditional logarithmic-type error transformation function, this paper adopts an arctangent-form error transformation function

$$h(s_i(t))=\begin{cases}\frac{2}{\pi}\bar{\delta}_i\arctan(s_i(t)) & s_i(t)\geqslant 0 \\ \frac{2}{\pi}\underline{\delta}_i\arctan(s_i(t)) & s_i(t)<0\end{cases} \tag{9}$$

where $s_i(t)$ is the transformed unconstrained error, and the transformation function parameter $h(\cdot)$ satisfies

$$\lim_{s_i(t)\to+\infty} h(s_i(t))=\bar{\delta}_i,\quad \lim_{s_i(t)\to-\infty} h(s_i(t))=-\underline{\delta}_i \tag{10}$$

According to Eq.(9), the equivalently transformed unconstrained error $s_i(t)$ can be derived as

$$s_i(t)=h^{-1}(\vartheta_i(t))=\begin{cases}\tan\left(\dfrac{\pi}{2}\dfrac{\vartheta_i(t)}{\bar{\delta}_i}\right) & \vartheta_i(t)\geqslant 0\\ \tan\left(\dfrac{\pi}{2}\dfrac{\vartheta_i(t)}{\underline{\delta}_i}\right) & \vartheta_i(t)<0\end{cases} \tag{11}$$

It can be seen that the transformed error satisfies $s_i(t)\in(-\infty,+\infty)$. To avoid singularities caused by the error exceeding the prescribed performance boundary, which would hinder accurate evaluation of system performance, a "barrier-crossing" error transformation function is introduced. This function allows the simulation to continue even when the error exceeds the boundary, providing more flexibility for adjustment in controller design.

### 2.2 Design of backstepping controller based on prescribed-time performance

Considering the fast initial response and slow terminal convergence of the backstepping method[26], this paper proposes a prescribed-time performance-based backstepping attitude controller. First, define the error variables $\boldsymbol{x}_1$ and $\boldsymbol{x}_2$

$$\begin{cases}\boldsymbol{x}_1=\boldsymbol{s}\\ \boldsymbol{x}_2=\boldsymbol{\omega}_{\mathrm{e}}-\boldsymbol{\alpha}\end{cases} \tag{12}$$

where $\boldsymbol{s}=[s_1\quad s_2\quad s_3]^{\mathrm{T}}$ and $\boldsymbol{\alpha}$ is the virtual control law.

The transformed attitude error dynamics of the spacecraft can then be expressed as

$$\begin{cases}\dot{\boldsymbol{x}}_1=\dot{\boldsymbol{s}}\\ \boldsymbol{J}\dot{\boldsymbol{x}}_2=\boldsymbol{J}\dot{\boldsymbol{\omega}}_{\mathrm{e}}-\boldsymbol{J}\dot{\boldsymbol{\alpha}}=\boldsymbol{C}_{\mathrm{r}}+\boldsymbol{u}-\boldsymbol{J}\dot{\boldsymbol{\alpha}}\end{cases} \tag{13}$$

where $\boldsymbol{C}_{\mathrm{r}}=-\boldsymbol{\omega}^{\times}\boldsymbol{J}\boldsymbol{\omega}+\boldsymbol{J}\boldsymbol{\omega}_{\mathrm{e}}^{\times}\boldsymbol{R}_{\mathrm{e}}\boldsymbol{\omega}_{\mathrm{d}}-\boldsymbol{J}\boldsymbol{R}_{\mathrm{e}}\dot{\boldsymbol{\omega}}_{\mathrm{d}}$.

For the second-order system, by constructing two Lyapunov functions, the controller is designed as follows

$$\boldsymbol{u}=-k_2\boldsymbol{x}_2-\boldsymbol{C}_{\mathrm{r}}+\boldsymbol{J}\dot{\boldsymbol{\alpha}}-\boldsymbol{x}_1^{\mathrm{T}} \tag{14}$$

where $k_2>0$ is a gain constant that adjusts the system's convergence speed, and $\boldsymbol{\alpha}$ is the virtual control law, defined as

$$\boldsymbol{\alpha}=-k_1\boldsymbol{x}_1+\boldsymbol{\omega}_{\mathrm{e}}-\dot{\boldsymbol{x}}_1 \tag{15}$$

where $k_1$ is a positive constant. Since $\boldsymbol{x}_1$ and $\boldsymbol{x}_2$ are bounded, choosing an appropriate value of $k_1$ to ensure system stability.

### 2.3 Design of disturbance observer

An adaptive disturbance observer based on the super-twisting algorithm[27] is designed to estimate the high-frequency compound disturbance caused by inertia uncertainty and external disturbance torques, thereby enhancing the robustness of the controller.

Given the states $\boldsymbol{q}$ and $\boldsymbol{\omega}$ of Eq.(2), and denoting the nonlinear compound disturbance as $\boldsymbol{D}$, let $\boldsymbol{r}_1=\boldsymbol{q}$, $\boldsymbol{r}_2=\boldsymbol{\omega}$, Eq.(2) is transformed into

$$\begin{cases}\dot{\boldsymbol{r}}_1=\dfrac{1}{2}(q_0\boldsymbol{E}_3+\boldsymbol{r}_1^{\times})\boldsymbol{r}_2=\dfrac{1}{2}g(\boldsymbol{r}_1)\boldsymbol{r}_2\\ \dot{\boldsymbol{r}}_2=\boldsymbol{B}+\boldsymbol{C}\boldsymbol{u}+\boldsymbol{D}\end{cases} \tag{16}$$

where $\boldsymbol{B}=-\boldsymbol{J}_0^{-1}\boldsymbol{r}_2^{\times}\boldsymbol{J}_0\boldsymbol{r}_2$, $\boldsymbol{D}=\boldsymbol{J}_0^{-1}(\boldsymbol{d}-\boldsymbol{r}_2^{\times}\Delta\boldsymbol{J}\boldsymbol{r}_2-\Delta\boldsymbol{J}\dot{\boldsymbol{r}}_2)$, $\boldsymbol{C}=\boldsymbol{J}_0^{-1}$ and the $\boldsymbol{D}$, composed of moment of inertia uncertainty and external disturbance torque, along with its first derivative $\dot{\boldsymbol{D}}$, are both bounded, that is $\|D_j\|\leqslant\bar{d}_1$, $\|\dot{D}_j\|\leqslant\bar{d}_2$, $j=1,2,3$.

Assuming the observed value of $\boldsymbol{r}_2$ is $\hat{\boldsymbol{r}}_2$, and the observed value of disturbance $\boldsymbol{D}$ is $\hat{\boldsymbol{D}}$, then

$$\dot{\hat{\boldsymbol{r}}}_2=\boldsymbol{B}+\boldsymbol{C}\boldsymbol{u}+\hat{\boldsymbol{D}} \tag{17}$$

Define the observer error as $\boldsymbol{e}=\boldsymbol{r}_2-\hat{\boldsymbol{r}}_2$. Based on the super-twisting algorithm, the disturbance observer is designed as follows

$$\hat{D}_j=\lambda_{1,j}(t)|e_j|^{1/2}\operatorname{sgn}(e_j)-\int\lambda_{2,j}(t)\operatorname{sgn}(e_j)\mathrm{d}t \tag{18}$$

where $\lambda_1(t)$ and $\lambda_2(t)$ are adaptive gains, with specific expressions given as follows

$$\begin{cases}\dot{\lambda}_{1,j}=\begin{cases}|\lambda_{1,j}|(|e_j|-\chi) & \lambda_{1,j}>\lambda_{\mathrm{m}}\\ \lambda_{\mathrm{m}} & \lambda_{1,j}\leqslant\lambda_{\mathrm{m}}\end{cases}\\ \lambda_{2,j}=\mu\lambda_{1,j}\end{cases} \tag{19}$$

where $\lambda_{\mathrm{m}},\chi,\mu$ are designed positive constants. If there exists positive constants $\varepsilon,\gamma$ such that Eq.(20) holds, then the observer error $\boldsymbol{e}$ will converge in finite time.

$$\lambda_{1,j}>\frac{(\varepsilon+\gamma+\mu^2)}{4\mu\gamma}-\frac{\varepsilon\mu}{\gamma} \tag{20}$$

Combining Eqs.(16, 17), the first-order derivative of the observation error can be expressed as

$$\dot{e}_j=D_j-\lambda_{1,j}|e_j|^{1/2}\operatorname{sgn}(e_j)+\int\lambda_{2,j}\operatorname{sgn}(e_j)\mathrm{d}t \tag{21}$$

### 2.4 Design of attitude cooperative controller

Furthermore, due to network transmission delays and attitude determination error, the attitude information $\boldsymbol{\omega}_i$ and $\boldsymbol{Q}_i$ received by the controllers of the two individual spacecraft are different. Based on consensus theory[28], an attitude cooperative control algorithm is introduced to ensure that the output torques of the two spacecraft in the combination remain synchronized. First, the following assumptions are made for the attitude cooperative control system described in this paper

**Assumption 1** The communication topology among individual spacecraft is described by a weighted undirected graph $\boldsymbol{G}$. In addition, each spacecraft's attitude information is measured by its own attitude determination system and transmitted to the controller via wireless network with different transmission delays $T_j$.

**Assumption 2** The attitude error information $\boldsymbol{q}_{\mathrm{e}i}$ and $\boldsymbol{\omega}_{\mathrm{e}i}$ computed by each controller is transmitted to other controllers via the wireless network. Let $T_{ij}$ denote the transmission delay from controller $i$ to controller $j$, and its derivative is bounded such that $\dot{T}_{ij} \leqslant \bar{t}_{ij}$.

Therefore, based on the above controller, the combined spacecraft attitude cooperative controller is designed as follows

$$\boldsymbol{\tau}_i = -k_2\boldsymbol{x}_2 - \boldsymbol{C}_{\mathrm{r}} + \boldsymbol{J}\dot{\boldsymbol{\alpha}} - \boldsymbol{x}_1^{\mathrm{T}} - \hat{\boldsymbol{D}} + \sum_{j=1}^{n} a_{ij}[c(\boldsymbol{q}_{\mathrm{e}i} - \boldsymbol{q}_{\mathrm{e}j}(t - T_{ij})) + h(\boldsymbol{\omega}_{\mathrm{e}i} - \boldsymbol{\omega}_{\mathrm{e}j}(t - T_{ij}))] \tag{22}$$

where $a_{ij}$ is an element of the adjacency matrix, and $T_{ij}$ the transmission delay from controller $i$ to controller $j$, assumed to be time-varying. $c$ and $h$ are the positive gain parameters.

### 2.5 Stability analysis

**Theorem 1** For the prescribed-time performance function in Eq. (8), if $\boldsymbol{p}_0 > \boldsymbol{p}_\infty > 0$ is satisfied, then the performance function $\boldsymbol{p}(t)$ will converge within the $T_{\mathrm{d}}$ to the specified steady-state accuracy $\boldsymbol{p}_\infty$.

**Proof** For the variable $\boldsymbol{p}(t) - \boldsymbol{p}_\infty$, define its Lyapunov function as $V_0(t) = (1/2)(\boldsymbol{p}(t) - \boldsymbol{p}_\infty)^2$. Combining with Eq. (8) and taking the derivative yields

$$\begin{aligned}
&\dot{V}_0(t) = (\boldsymbol{p}(t) - \boldsymbol{p}_\infty)\dot{\boldsymbol{p}}(t) = \\
&\quad (\boldsymbol{p}(t) - \boldsymbol{p}_\infty)\left[-\frac{(\boldsymbol{p}_0 - \boldsymbol{p}_\infty)}{(1-k)T_{\mathrm{d}}}(1 - t/T_{\mathrm{d}})^{\frac{k}{1-k}}\right] = \\
&\quad (\boldsymbol{p}(t) - \boldsymbol{p}_\infty)\left[-\frac{(\boldsymbol{p}_0 - \boldsymbol{p}_\infty)}{(1-k)T_{\mathrm{d}}}\left(\frac{(\boldsymbol{p}(t) - \boldsymbol{p}_\infty)}{(\boldsymbol{p}_0 - \boldsymbol{p}_\infty)}\right)^k\right] = \\
&\quad -\frac{(\boldsymbol{p}_0 - \boldsymbol{p}_\infty)^{1-k}}{(1-k)T_{\mathrm{d}}}(\boldsymbol{p}(t) - \boldsymbol{p}_\infty)^{k+1} = \\
&\quad -2^{\frac{k+1}{2}}\xi(t)V_0^{\frac{k+1}{2}}(t)
\end{aligned} \tag{23}$$

where function $\xi$ represents $\xi(t) = (\boldsymbol{p}_0 - \boldsymbol{p}_\infty)^{1-k}/(1-k)T_{\mathrm{d}}$. For $(k+1)/2 \in (0, 1)$, according to Theorem 4.2 in Ref.[29], when time $t$ satisfies

$$t \geqslant T_{\mathrm{d}} = \frac{(\boldsymbol{p}_0 - \boldsymbol{p}_\infty)^{1-k}}{\xi(t)(1-k)} \tag{24}$$

Then the variable $(\boldsymbol{p}(t) - \boldsymbol{p}_\infty)$ tends to zero. In other words, the prescribed performance function $\boldsymbol{p}(t)$ converges to its final value $\boldsymbol{p}_\infty$ before time $T_{\mathrm{d}}$, and remains equal to $\boldsymbol{p}_\infty$ thereafter.

For the stability proof of the disturbance observer, assume the existence of two intermediate variables $H \in \mathbf{R}^{3\times 1}$, $K \in \mathbf{R}^{3\times 1}$, and let $\boldsymbol{\beta}_j = [H_j \quad K_j]^{\mathrm{T}}, j = 1, 2, 3$. Its specific form is as follows

$$\boldsymbol{\beta}_j = \begin{bmatrix} H_j \\ K_j \end{bmatrix} = \begin{bmatrix} |e_j|^{1/2}\operatorname{sgn}(e_j) \\ D_j - \int \lambda_{2,j}(t)\operatorname{sgn}(e_j)\mathrm{d}t \end{bmatrix} \tag{25}$$

Taking the derivative of the above expression yields

$$\dot{\boldsymbol{\beta}}_j = \begin{bmatrix} \dot{H}_j \\ \dot{K}_j \end{bmatrix} = \begin{bmatrix} \dfrac{K_j - \lambda_{1,j}H_j}{2|H_j|} \\ \dot{D}_j - \lambda_{2,j}\operatorname{sgn}(e_j) \end{bmatrix} \tag{26}$$

Since $\|\dot{D}_j\| \leqslant \bar{d}_2$ and there exists a constant $\eta$ such that $0 < \eta < 2\bar{d}_2$, $\dot{D}_j$ can be expressed as

$$\dot{D}_j = \frac{\eta}{2}\operatorname{sgn}(e_j) = \frac{\eta}{2}\frac{H_j}{|H_j|} \tag{27}$$

Substituting Eq.(27) into Eq.(26) can obtain

$$\dot{\boldsymbol{\beta}}_j=\begin{bmatrix}\dfrac{K_j-\lambda_{1,j}H_j}{2|H_j|}\\ \dot{D}_j-\lambda_{2,j}\operatorname{sgn}(e_j)\end{bmatrix}=\frac{1}{2|H_j|}\begin{bmatrix}-\lambda_{1,j} & 1\\ \eta-\lambda_{2,j} & 0\end{bmatrix}\begin{bmatrix}H_j\\ K_j\end{bmatrix}=\boldsymbol{F\beta}_j \tag{28}$$

For the variable $\boldsymbol{\beta}_j$, design the Lyapunov function in the following form

$$V_j=\boldsymbol{\beta}_j^{\mathrm{T}}\boldsymbol{P\beta}_j=\boldsymbol{\beta}_j^{\mathrm{T}}\begin{bmatrix}\gamma+\mu^2 & -\mu\\ -\mu & 1\end{bmatrix}\boldsymbol{\beta}_j \tag{29}$$

where $\boldsymbol{P}$ is a positive definite matrix.

Differentiating Eq.(29) yields

$$\begin{aligned}\dot{V}_j=&\dot{\boldsymbol{\beta}}_j^{\mathrm{T}}\boldsymbol{P\beta}_j+\boldsymbol{\beta}_j^{\mathrm{T}}\boldsymbol{P}\dot{\boldsymbol{\beta}}_j=\boldsymbol{\beta}_j^{\mathrm{T}}(\boldsymbol{F}^{\mathrm{T}}\boldsymbol{P}+\boldsymbol{PF})\boldsymbol{\beta}_j=\\ &-\frac{1}{2|H_j|}\boldsymbol{\beta}_j^{\mathrm{T}}\begin{bmatrix}2\lambda_{1,j}\gamma+2\mu\eta & -\eta-\gamma-\mu^2\\ -\eta-\gamma-\mu^2 & 2\mu\end{bmatrix}\boldsymbol{\beta}_j=\\ &-\frac{1}{2|H_j|}\boldsymbol{\beta}_j^{\mathrm{T}}\boldsymbol{Q\beta}_j\end{aligned} \tag{30}$$

If appropriate parameters are chosen such that the minimum eigenvalue of matrix $\boldsymbol{Q}$ satisfies $\det_{\min}(\boldsymbol{Q})\geqslant\mu$, then

$$\dot{V}_j=-\frac{1}{2|H_j|}\boldsymbol{\beta}_j^{\mathrm{T}}\boldsymbol{Q\beta}_j\leqslant-\frac{\mu}{2|H_j|}\|\boldsymbol{\beta}_j\|^2 \tag{31}$$

Similarly, for Eq.(29), we have

$$\det_{\min}(\boldsymbol{P})\|\boldsymbol{\beta}_j\|^2\leqslant V_j=\boldsymbol{\beta}_j^{\mathrm{T}}\boldsymbol{P\beta}_j\leqslant\det_{\max}(\boldsymbol{P})\|\boldsymbol{\beta}_j\|^2 \tag{32}$$

Since $|H_j|\leqslant\|\boldsymbol{\beta}_j\|\leqslant V_j^{1/2}/\det_{\min}^{1/2}(\boldsymbol{P})$, combining the above equations

$$\begin{aligned}\dot{V}_j\leqslant&-\frac{\mu}{2|H_j|}\|\boldsymbol{\beta}_j\|^2\leqslant-\frac{\mu}{2}\frac{\det_{\min}^{1/2}(\boldsymbol{P})}{V_j^{1/2}}\|\boldsymbol{\beta}_j\|^2\leqslant\\ &-\frac{\mu}{2}\frac{\det_{\min}^{1/2}(\boldsymbol{P})}{\det_{\max}(\boldsymbol{P})}V_j^{1/2}\leqslant-\rho V_j^{1/2}\end{aligned} \tag{33}$$

From the above equation, it can be seen that the finite-time stability condition given in Lemma 1 of Ref.[27] is satisfied.

In addition, to prove the stability of the robust cooperative controller with prescribed-time convergence that proposed in this paper, the Lyapunov function is designed in the following form

$$\begin{aligned}V^k=&V_1+V_2=\frac{1}{2}\boldsymbol{x}_1^{\mathrm{T}}\boldsymbol{x}_1+\frac{1}{2}\boldsymbol{x}_2^{\mathrm{T}}\boldsymbol{Jx}_2+\frac{1}{2}\sum_{i=1}^{n}\boldsymbol{z}_i^{\mathrm{T}}\boldsymbol{Jz}_i+\\ &\frac{1}{2}\sum_{i=1}^{n}\sum_{j=1}^{n}b_{ij}\int_{t-T_{ij}}^{t}\boldsymbol{z}_j^{\mathrm{T}}(\sigma)\boldsymbol{z}_j(\sigma)\mathrm{d}\sigma\end{aligned} \tag{34}$$

where $b_{ij}$ is a positive gain parameter. From Eq.(14) and Eq.(15), the derivative of $V_1$ is given by

$$\begin{aligned}\dot{V}_1=&\boldsymbol{x}_1^{\mathrm{T}}\dot{\boldsymbol{x}}_1+\boldsymbol{x}_2^{\mathrm{T}}\boldsymbol{J}\dot{\boldsymbol{x}}_2=\\ &\boldsymbol{x}_1^{\mathrm{T}}(\dot{\boldsymbol{x}}_1-\boldsymbol{\omega}_{\mathrm{e}}+\boldsymbol{x}_2+\boldsymbol{\alpha})+\boldsymbol{x}_2^{\mathrm{T}}(\boldsymbol{C}_{\mathrm{r}}+\boldsymbol{u}-\boldsymbol{J}\dot{\boldsymbol{\alpha}})=\\ &\boldsymbol{x}_1^{\mathrm{T}}(-k_1\boldsymbol{x}_1+\boldsymbol{x}_2)+\boldsymbol{x}_2^{\mathrm{T}}(-k_2\boldsymbol{x}_2-\boldsymbol{x}_1^{\mathrm{T}})=\\ &-k_1\boldsymbol{x}_1^{\mathrm{T}}\boldsymbol{x}_1-k_2\boldsymbol{x}_2^{\mathrm{T}}\boldsymbol{x}_2+\boldsymbol{x}_1^{\mathrm{T}}\boldsymbol{x}_2-\boldsymbol{x}_2^{\mathrm{T}}\boldsymbol{x}_1^{\mathrm{T}}=\\ &-k_1\boldsymbol{x}_1^{\mathrm{T}}\boldsymbol{x}_1-k_2\boldsymbol{x}_2^{\mathrm{T}}\boldsymbol{x}_2<0\end{aligned} \tag{35}$$

Let $\boldsymbol{z}_i=c\boldsymbol{q}_{\mathrm{e}i}+h\boldsymbol{\omega}_{\mathrm{e}i}$, differentiating the Lyapunov function $V_2$, related to the attitude cooperative controller parameters can obtain

$$\begin{aligned}\dot{V}_2=&\sum_{i=1}^{n}\boldsymbol{z}_i^{\mathrm{T}}\boldsymbol{J}\dot{\boldsymbol{z}}_i+\frac{1}{2}\sum_{i=1}^{n}\sum_{j=1}^{n}b_{ij}\boldsymbol{z}_j^{\mathrm{T}}\boldsymbol{z}_j-\\ &\frac{1}{2}\sum_{i=1}^{n}\sum_{j=1}^{n}b_{ij}(1-\dot{T}_{ij})\boldsymbol{z}_j^{\mathrm{T}}(t-T_{ij})\boldsymbol{z}_j(t-T_{ij})\end{aligned} \tag{36}$$

Substituting Eq.(6) and Eq.(22) can obtain

$$\begin{aligned}\dot{V}_2=&-\sum_{i=1}^{n}k_i\boldsymbol{z}_i^{\mathrm{T}}\boldsymbol{z}_i-\sum_{i=1}^{n}\sum_{j=1}^{n}a_{ij}\boldsymbol{z}_i^{\mathrm{T}}\boldsymbol{z}_i+\\ &\sum_{i=1}^{n}\sum_{j=1}^{n}a_{ij}\boldsymbol{z}_i^{\mathrm{T}}\boldsymbol{z}_j(t-T_{ij})+\frac{1}{2}\sum_{i=1}^{n}\sum_{j=1}^{n}b_{ij}\boldsymbol{z}_j^{\mathrm{T}}\boldsymbol{z}_j-\\ &\frac{1}{2}\sum_{i=1}^{n}\sum_{j=1}^{n}b_{ij}(1-\dot{T}_{ij})\boldsymbol{z}_j^{\mathrm{T}}(t-T_{ij})\boldsymbol{z}_j(t-T_{ij})\end{aligned} \tag{37}$$

From the basic inequality, it follows that

$$\boldsymbol{z}_i^{\mathrm{T}}\boldsymbol{z}_j(t-T_{ij})\leqslant\frac{1}{2}\boldsymbol{z}_i^{\mathrm{T}}\boldsymbol{z}_i+\frac{1}{2}\boldsymbol{z}_j^{\mathrm{T}}(t-T_{ij})\boldsymbol{z}_j(t-T_{ij}) \tag{38}$$

Additionally, considering $a_{ij}=a_{ji}$, it follows that

$$\sum_{i=1}^{n}\sum_{j=1}^{n}b_{ij}\boldsymbol{z}_i^{\mathrm{T}}\boldsymbol{z}_i=\sum_{i=1}^{n}\sum_{j=1}^{n}b_{ij}\boldsymbol{z}_j^{\mathrm{T}}\boldsymbol{z}_j \tag{39}$$

Since $\dot{T}_{ij}\leqslant\bar{t}_{ij}$, then

$$\begin{aligned}\dot{V}_2\leqslant&-\sum_{i=1}^{n}k_i\boldsymbol{z}_i^{\mathrm{T}}\boldsymbol{z}_i-\frac{1}{2}\sum_{i=1}^{n}\sum_{j=1}^{n}(a_{ij}-b_{ij})\boldsymbol{z}_i^{\mathrm{T}}\boldsymbol{z}_i-\\ &\frac{1}{2}\sum_{i=1}^{n}\sum_{j=1}^{n}(b_{ij}(1-\bar{t}_{ij})-a_{ij})\boldsymbol{z}_j^{\mathrm{T}}(t-T_{ij})\boldsymbol{z}_j(t-T_{ij})\end{aligned} \tag{40}$$

Provided that $b_{ij}(1-\bar{t}_{ij})\geqslant a_{ij}$ and $a_{ij}\geqslant b_{ij}$, it follows that

$$\dot{V}_2\leqslant-\sum_{i=1}^{n}k_i\boldsymbol{z}_i^{\mathrm{T}}\boldsymbol{z}_i \tag{41}$$

Consequently, $\dot{V}^k=\dot{V}_1+\dot{V}_2<0$. It indicates that the subsystem corresponding to the individual controller is stable. Construct the overall Lyapunov function

$$V=\sum_{k=1}^{n}V^{k} \tag{42}$$

Given that the orthogonality of the transformation matrix $\boldsymbol{R}_k^{\mathrm{b}}$ ensures the boundedness of state transmission, differentiating $V$ and substitute the overall control law Eq.(3) can obtain

$$\dot{V}=\sum_{k=1}^{n}\dot{V}^{k}\leqslant-\sum_{k=1}^{n}\alpha_k\|\boldsymbol{x}_k\|^2 \tag{43}$$

Connected inter-subsystem communication topology ensures state coordination, prevents error accumulation in locally isolated subsystems, and ultimately guarantees overall system stability. This completes the proof.

## 3 Numerical Simulation and Analysis

### 3.1 Simulation parameters

The moment of inertia matrix $\boldsymbol{J}_0$ of the combined spacecraft is given by $\boldsymbol{J}_0=\mathrm{diag}[70\ 70\ 50]\,\mathrm{kg\cdot m^2}$. The actual moment of inertia matrix is denoted as $\boldsymbol{J}=\boldsymbol{J}_0+\Delta\boldsymbol{J}$, where $\Delta\boldsymbol{J}=0.1\sin(0.3t)\boldsymbol{J}_0$ represents the inertia uncertainty.

First, considering the actuator output is bounded, the maximum output torque is set to 0.2 N•m. The initial attitude angle of the spacecraft is set to $[20°\ 15°\ -20°]^{\mathrm{T}}$ with an initial angular velocity of $[0\ 0\ 0]^{\mathrm{T}}$; the target attitude angle and angular velocity are both set to $[0\,0\,0]^{\mathrm{T}}$ and $[0\ 0\ 0]^{\mathrm{T}}$. In addition, it is simply assumed that the relative attitude angle between the two separate spacecraft is $[0\ 0\ 0]^{\mathrm{T}}$. The simulation also considers attitude determination errors and external disturbance torques acting on the combined spacecraft. The specific parameter settings are as follows. The attitude angle measurement error is on the order of 0.000 1°, the angular velocity measurement error is on the order of 0.000 1 (°)/s, and the external disturbance torque is $10^{-3}$ N•m.

For the purpose of simulating a real-world wireless network transmission environment, the transmission delays from each attitude sensor to the controller are set as $T_1=0.02$ s, $T_2=0.03$ s. In addition, The network transmission delays for data exchange between the controllers of the combined spacecraft are set as

$$\begin{cases}T_{12}=0.01+0.02\sin(0.2t)\\T_{21}=0.01+0.02\cos(0.1t)\end{cases}$$

The relevant parameters of the disturbance observer are as follows: $\mu=0.2$, $\chi=1.5\times10^{-4}$, $\lambda_{\mathrm{m}}=0.003$, $\lambda_{1,j}(0)=0.03$。

In addition, the specific parameters of the two controllers are listed in Table 1.

**Table 1 Controller parameters**

| Parameter | Value |
|---|---|
| Initial value and final value | $p_{i,0}=0.25$, $p_{i,\infty}=0.001$ |
| Predefined time/s | $T_{\mathrm{d}}=30,40,50,60$ |
| Convergence rate constant | $k=0.4$ |
| Controller gain constant | $k_1=0.05$, $k_2=9.5$ |
| Adjacency matrix gain | $c=1$, $h=0.2$ |

### 3.2 Simulation results and analysis

To verify the effectiveness and stability of the proposed prescribed time attitude cooperative controller based on disturbance observer (PTCDO) under external disturbances such as inertia uncertainty and communication delays, numerical simulations are conducted using the parameters defined above. First, four different predefined convergence times are set: 30, 40, 50 and 60 s. The corresponding simulation results are shown in Figs.3—5. Then, a comparative study is performed with the proportional derivative (PD) control, the backstepping control (BP) and the prescribed time attitude cooperative control with adaptive disturbance rejection (PTCADR) [30]. The results are presented in Figs.6—8.

As can be seen from the results in Fig.3 and Fig.4, the combined spacecraft can accurately converge to the target attitude at the corresponding angular velocity within the prescribed time in the presence of inertia uncertainties, communication delays and external disturbances. All curves remain within the prescribed performance bounds, with favorable dynamic performance and robustness, and the specific control accuracy is listed in Table 2.

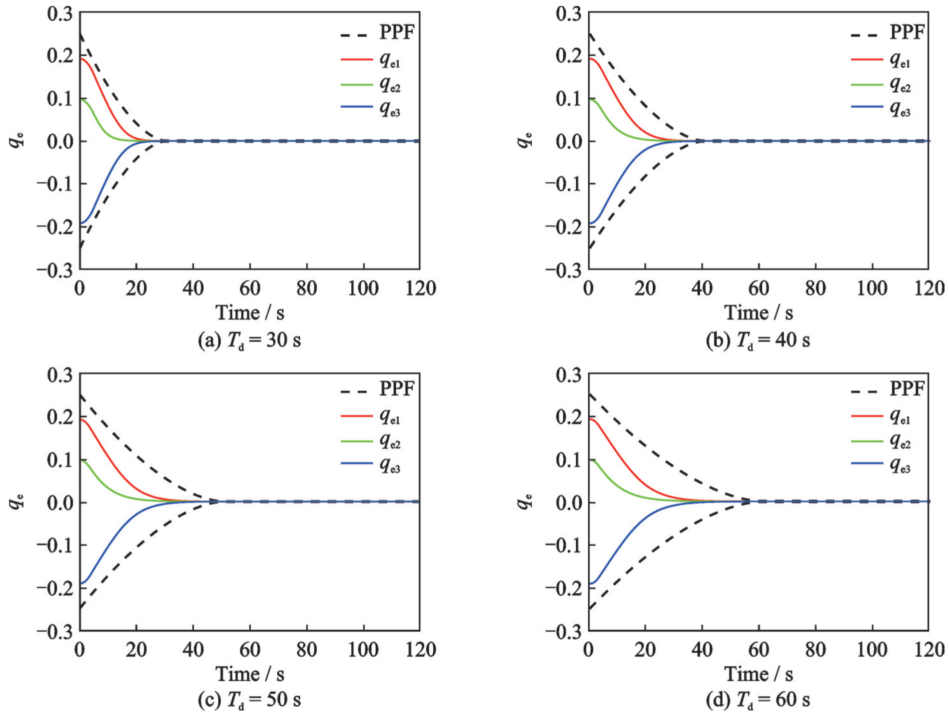


Fig.3 Error quaternion curves

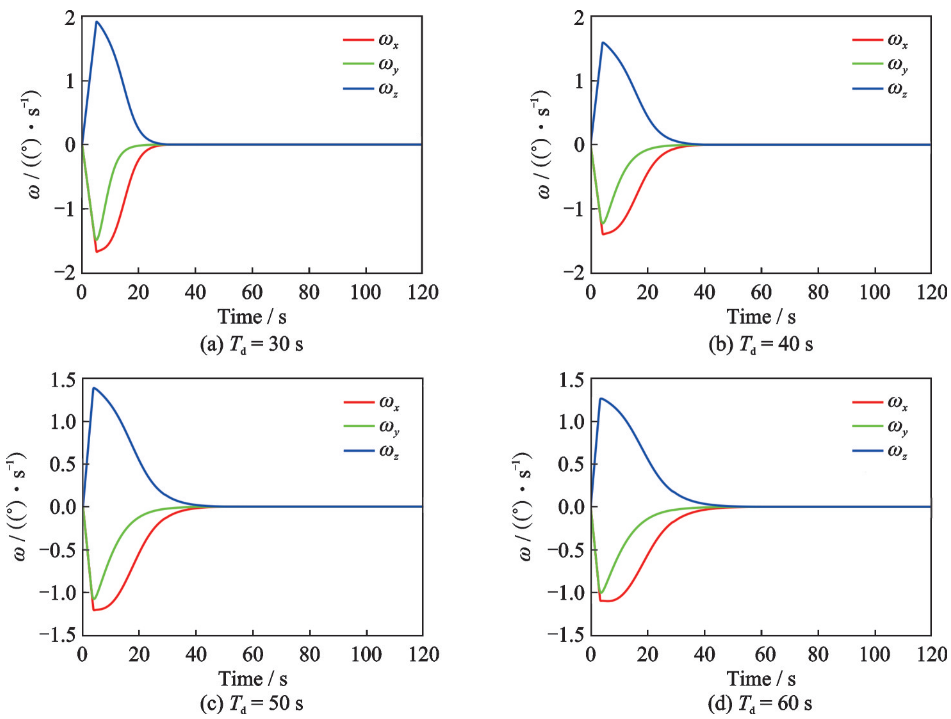


Fig.4 Angular velocity curves

Furthermore, the time response curves of the control torque presented in Fig.5 reveals a clear correlation between the output characteristics of the control torque and the prescribed convergence time: The shorter the prescribed convergence time, the larger the control torque output by the controller. This observation aligns with the objective principle that rapid dynamic adjustment inevitably relies on a larger control input to provide sufficient angular acceleration. Therefore, the prescribed time performance control method proposed in this paper is effective, which allows users to set the system convergence time according to mission requirements and thus exhibits excellent engineering application value.

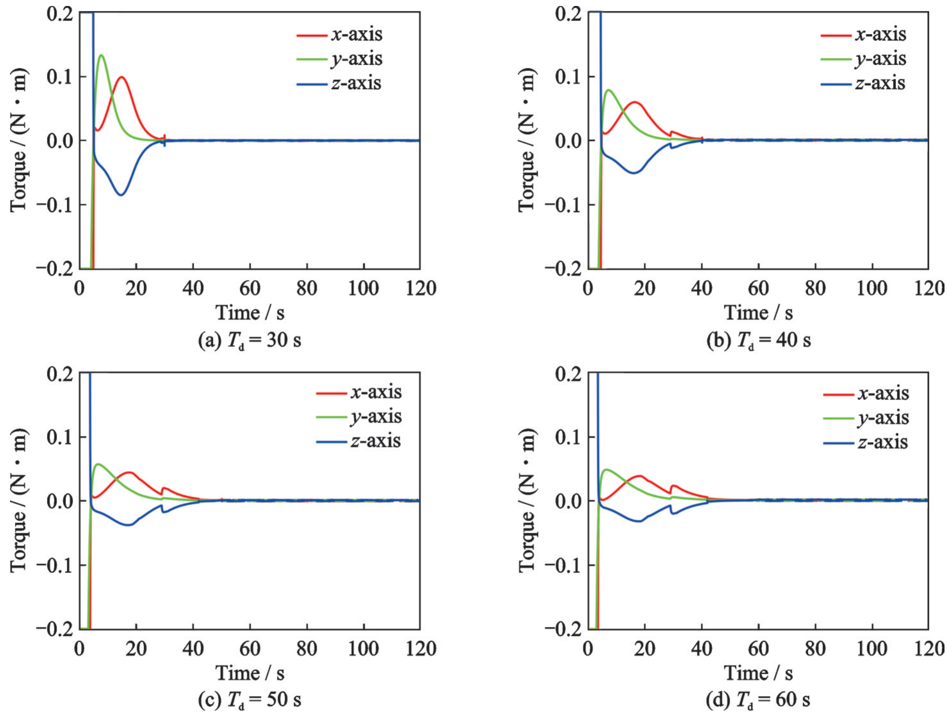


Fig.5 Control torque curves

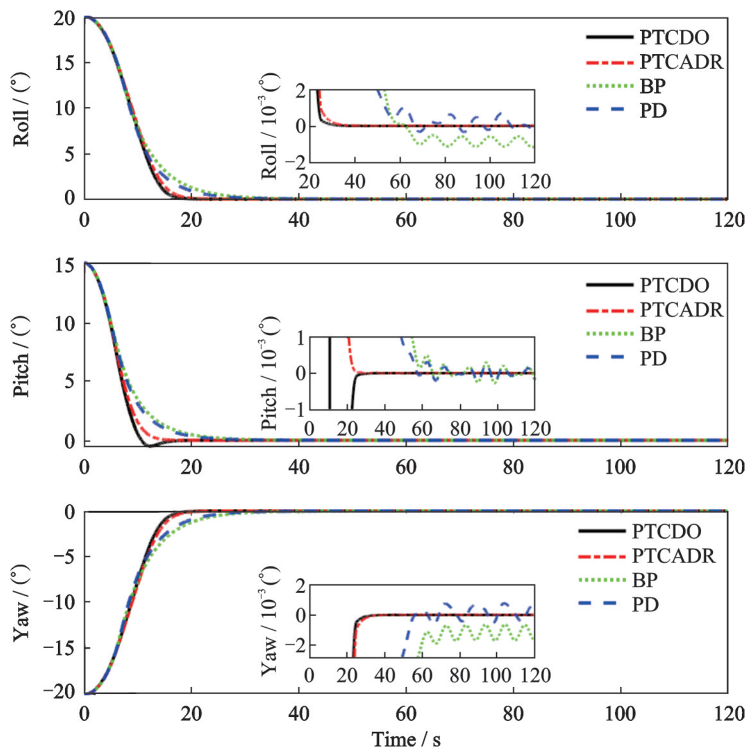


Fig.6 Euler angle curves

Figs.6—8 show the comparative simulation results of four control methods. As illustrated, compared with PD and BP controllers, the proposed PTCDO controller exhibits superior attitude control performance under challenging conditions such as inertia uncertainty, communication delay and other external disturbances. Benefiting from the strict constraint imposed by the prescribed time performance function, the controller not only ensures rapid convergence of the attitude error within a prescribed time, thereby significantly improving the response speed of attitude maneuvering, but also effectively

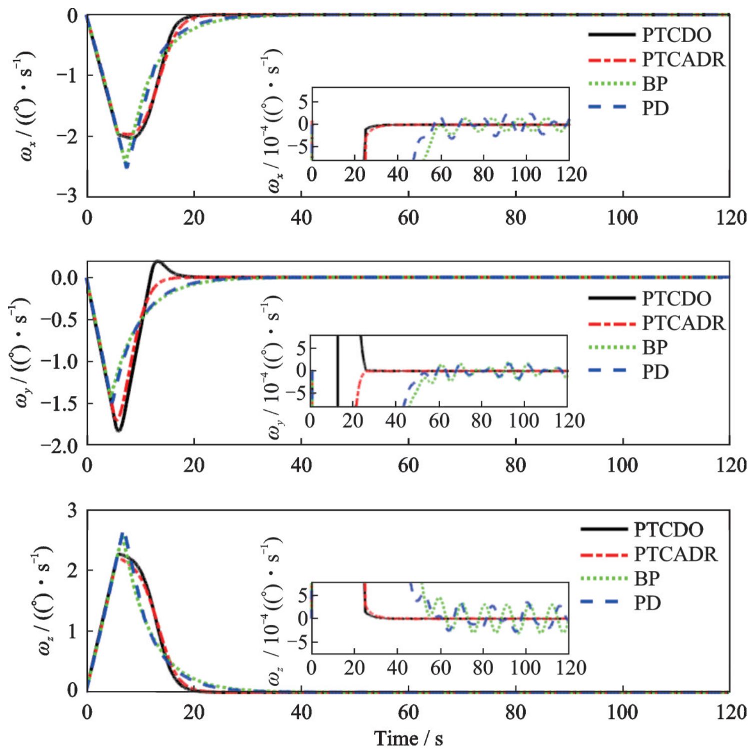


Fig.7 Angular velocity curves

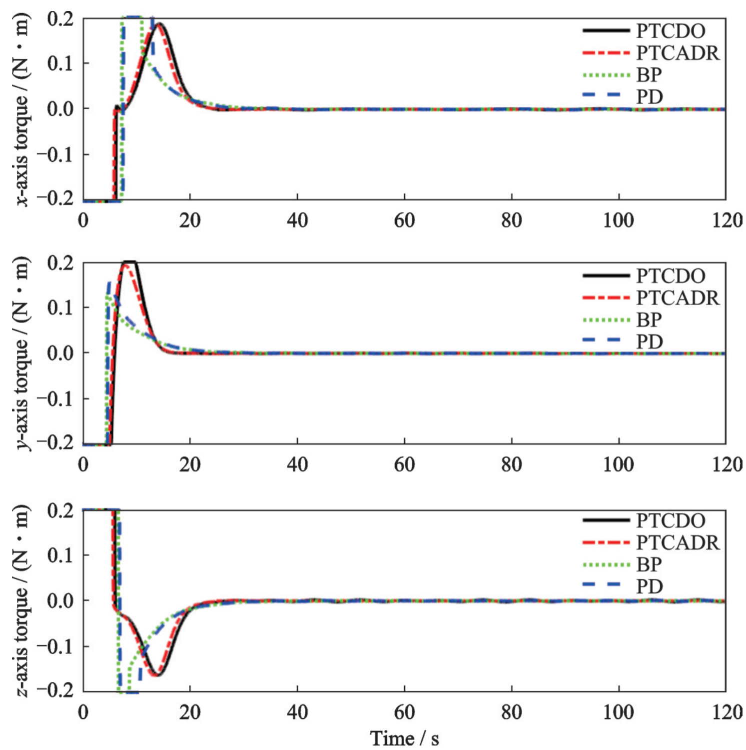


Fig.8 Control torque curves

**Table 2 Comparison of simulation results**

| Parameter | PTCDO | PTCADR | BP | PD |
|---|---|---|---|---|
| Attitude angle accuracy/$10^{-4}$(°) | 2 | 4 | 0.1 | 8 |
| Angular velocity accuracy/ $10^{-4}$((°)•s$^{-1}$) | 1.2 | 2 | 5 | 4 |
| Convergence time/s | 25 | 25 | 48 | 45 |

suppresses the influence of various disturbances, resulting in higher control accuracy. Further comparison with the PTCADR controller employing adaptive passive disturbance rejection demonstrates that, by virtue of the active estimation capability of the disturbance observer, the PTCDO controller can accurately identify and dynamically compensate for the composite disturbances arising from inertia perturbations and external disturbance torques. Consequently, the adverse effects of disturbances on the control system are fundamentally mitigated, leading to enhanced robustness and improved control precision. Detailed comparisons of convergence time and control accuracy among the considered controllers are summarized in Table 2.

As shown in Fig.9 and Fig.10, the disturbance observer based on the super-twisting algorithm can rapidly estimate the composite disturbance after a short transient chattering phase. Moreover, the attitude cooperative control term $\tau_e$ effectively compensates for attitude information inconsistency caused by attitude determination errors and communication delays, thereby enhancing the controller's robustness against external disturbances.

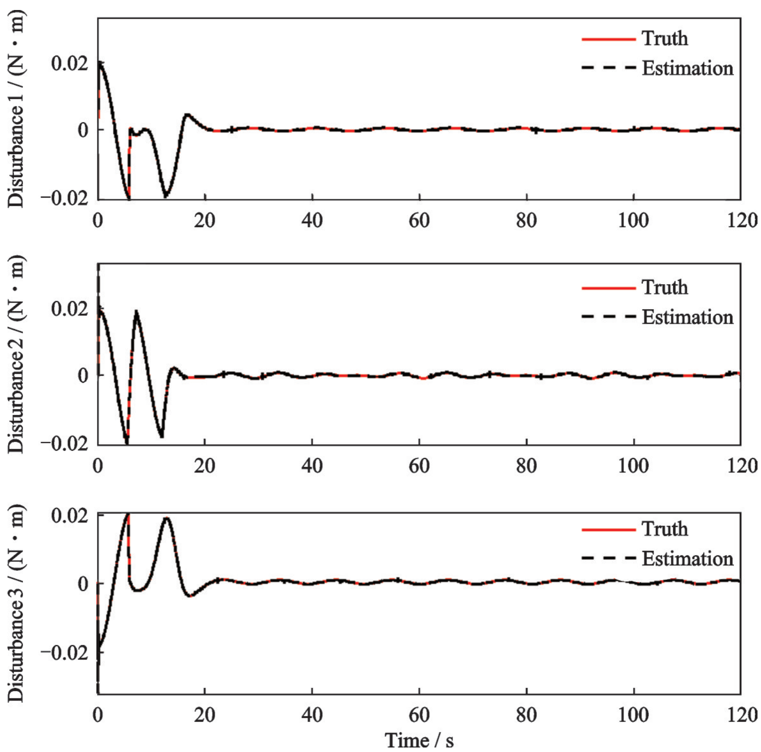


Fig.9 Estimated value of composite disturbance

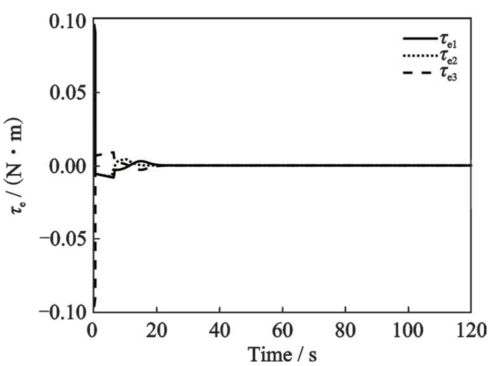


Fig.10 Cooperative control term

Based on the above simulation results, compared with other three control methods, the prescribed time attitude cooperative control methods based on disturbance observer allows the convergence time to be directly specified by the user and exhibits stronger robustness against external disturbances, thanks to the combined effect of the disturbance observer and the bounds of the prescribed time performance function. In addition, the system's steady-state error is always confined within the terminal value of the prescribed performance function, resulting in faster convergence and higher control accuracy.

## 4 Conclusions

This paper focuses on the prescribed time attitude cooperative control problem for combined spacecraft under external disturbances such as inertia uncertainty and communication delays. Firstly, a novel predefined-time performance function and a penetration-enabled error transformation function are proposed. Compared with traditional exponential-type performance functions, the proposed method achieves faster convergence, allows predefined convergence time and simplifies parameter tuning. Secondly, based on backstepping control theory, a predefined-time attitude controller for combined spacecraft is developed ensuring that the system states enter a predefined stability domain within the desired convergence time. Meanwhile, a disturbance observer based on the super-twisting algorithm is introduced to estimate the compound disturbance caused by inertia uncertainty and external torques. A cooperative control term is designed using consensus theory to compensate for the control torque mismatch induced by communication delays, enhancing the robustness of the controller. Finally, a series of comparative simulations are conducted to demonstrate the effectiveness and superiority of the proposed controller.

**References**


[1] MAO Y H, WU Y H, JU X Z, et al. Dynamic management topology construction, evolution, and maintenance of low earth orbit mega-constellation[J]. Space: Science & Technology, 2025, 5: 248.

[2] WU Y H, YU Z C, LI C Y, et al. Reinforcement learning in dual-arm trajectory planning for a free-floating space robot[J]. Aerospace Science and Technology, 2020, 98: 105657.

[3] WU Y H, HE M J, YU Z C, et al. Dynamics modeling and attitude stabilization control of a multiarmed space robot for on-orbit servicing[J]. Journal of the Franklin Institute, 2020, 357(13): 8383-8415.

[4] YU Binggu, WANG Shuquan. Reconfiguration of spacecraft cluster based on distributed local information[J]. Transactions of Nanjing University of Aeronautics and Astronautics, 2021, 38(4): 704-712.

[5] WU Jiaqi, KANG Guohua, HUA Yinmiao, et al. Research on intelligent cooperative attitude control of assembled spacecraft[J]. Chinese Space Science and Technology, 2020, 40(4): 44-53. (in Chinese)

[6] XU Y Q, HU Q L, SHAO X D. Composite adaptive attitude control for combined spacecraft with inertia uncertainties[J]. Aerospace Science and Technology, 2022, 131: 107984.

[7] ZHANG J, HU Q L, WANG D W, et al. Robust attitude coordinated control for spacecraft formation with communication delays[J]. Chinese Journal of Aeronautics, 2017, 30(3): 1071-1085.

[8] HUANG P F, WANG D K, ZHANG F, et al. Postcapture robust nonlinear control for tethered space robot with constraints on actuator and velocity of space tether[J]. International Journal of Robust and Nonlinear Control, 2017, 27(16): 2824-2841.

[9] WANG D, WU Y H, XIE H Y, et al. Scheduled input shaping based attitude agile control for flexible spacecraft with vibration suppression[J]. Aerospace Science and Technology, 2025, 164: 110355.

[10] WANG D, WU Y H, YUE C F, et al. Fully actuated system-based active disturbance rejection saturated attitude control for flexible spacecraft[J]. Journal of the Franklin Institute, 2025, 362(6): 107613.

[11] ZHANG C X, LU W J, ZHAO S Y, et al. Enhancing attitude tracking with self-learning control using tanh-type learning intensity[J]. IEEE Transactions on Automation Science and Engineering, 2025, 22: 16976-16986.

[12] YIN T L, ZHANG C X, WANG J H, et al. Configuration maintenance in multisatellite orbits via co-phase and control optimization[J]. IEEE Transactions on Aerospace and Electronic Systems, 2025, 61(6): 16738-16750.

[13] XING Y P, SONG Y S, YIN Z Y, et al. Exponential attitude-orbit coordinated control for gravitational-wave detection spacecraft formation with large-scale communication delays[J]. Transactions of Nanjing University of Aeronautics and Astronautics, 2025, 42(1): 70-79.

[14] QIN Jiahu, MA Qichao, LI Man, et al. Recent advances on multi-agent collaboration: A cross-perspective of game and control theory[J]. Acta Automatica Sinica, 2025, 51(3): 489-509. (in Chinese)

[15] HAN Liang, REN Zhang, DONG Xiwang, et al. Research on cooperative control method and application for multiple unmanned aerial vehicles[J]. Navigation Positioning and Timing, 2018, 5(4): 1-7. (in Chinese)

[16] LIU Z L, YAN W S, ZHANG S X. Research on cooperative output regulation problem of multi-agent systems with time-varying delay under dynamic topology[J]. Journal of Northwestern Polytechnical University, 2019, 37(3): 479-487.

[17] BECHLIOULIS C P, ROVITHAKIS G A. Robust adaptive control of feedback linearizable MIMO nonlinear systems with prescribed performance[J]. IEEE Transactions on Automatic Control, 2008, 53(9): 2090-2099.

[18] LI X L, LUO X Y, WANG J G, et al. Finite-time consensus of nonlinear multi-agent system with prescribed performance[J]. Nonlinear Dynamics, 2018, 91(4): 2397-2409.

[19] HUA C C, CHEN J N, LI Y F. Leader-follower finite-time formation control of multiple quadrotors with prescribed performance[J]. International Journal of Systems Science, 2017, 48(12): 2499-2508.

[20] MENG Q R, LIN Y. Adaptive admittance tracking control for interactive robot with prescribed performance[J]. Journal of Systems Engineering and Electronics, 2024, 35(2): 444-450.

[21] GAO B L, WANG L Y, LI S Y, et al. Cloud-based predictive adaptive cruise control considering preceding vehicle and slope information[J]. Journal of Systems Engineering and Electronics, 2024, 35(6): 1542-1562.

[22] HAO Yong, JIA Denghui, LI Chenyang, et al. Event trigger-based prescribed-time tracking control of spacecraft[J]. CAAI Transactions on Intelligent Systems, 2024, 19(3): 661-669. (in Chinese)

[23] GAO S H, LIU X P, JING Y W, et al. A novel finite-time prescribed performance control scheme for spacecraft attitude tracking[J]. Aerospace Science and Technology, 2021, 118: 107044.

[24] HAN Nan, LUO Jianjun, MA Weihua. Concurrent learning cooperative game control for attitude takeover of failed satellites[J]. Acta Aeronautica et Astronautica Sinica, 2021, 42(3): 324307. (in Chinese)

[25] JIA Q X, LI G H, YU D, et al. Learning Chebyshev neural network-based spacecraft attitude tracking control ensuring finite-time prescribed performance[J]. Aerospace Science and Technology, 2024, 148: 109085.

[26] ZHANG Hong, WU Yunhua, ZHONG Shengjun, et al. Space target compound pointing control method based on backstepping[J]. Systems Engineering and Electronics, 2023, 45(9): 2884-2893. (in Chinese)

[27] ZHANG W, YUN W J, GUO Y N, et al. Super-twisting disturbance observer based finite-time attitude control for combined spacecraft[C]//Proceedings of 2020 Chinese Control and Decision Conference (CCDC). Hefei, China: IEEE, 2020: 267-271.

[28] BI Peng, LUO Jianjun, ZHANG Bo. Cooperative control algorithm for spacecraft formation flying based on consensus theory[J]. Journal of Astronautics, 2010, 31(1): 70-74. (in Chinese)

[29] BHAT S P, BERNSTEIN D S. Finite-time stability of continuous autonomous systems[J]. SIAM Journal on Control and Optimization, 2000, 38(3): 751-766.

[30] LI Wenxing, WU Yunhua, ZHU Yi, et al. Coordinated attitude control of spacecraft based on distributed intelligent actuators[J]. Journal of Harbin Engineering University, 2022, 43(5): 639-648. (in Chinese)

**Acknowledgement** This work was supported by the National Natural Science Foundation of China (No. 12572054).

**Authors**

**The first author** Mr. **ZHANG Hao** is an M.S. candidate at the College of Astronautics, Nanjing University of Aeronautics and Astronautics. His main research interests include spacecraft attitude dynamics and control, as well as hardware-in-the-loop simulation.

**The corresponding authors**

Prof. **WU Yunhua** is a professor at the Collge of Astronautics, Nanjing University of Aeronautics and Astronautics. He received his Ph.D. degree from Harbin Institute of Technology in 2008. His research interest covers attitude-orbit dynamics and control and spacecra-ft hardware-in-the-loop simulation.

Dr. **LU Zhenkun** is currently a lecturer in robotics engineering at Wenzhou University of Technology. He received his B.S. degree from Dalian Polytechnic University, M.S. degree from Shenyang Aerospace University and Ph.D. degree from Sun Yat-sen University. His research focuses on aircraft and intelligent robotic systems, including aircraft formation dynamics and control, robot navigation and path planning, intelligent perception and target recognition, and human-robot collaborative task optimization.

**Author contributions** Mr. **ZHANG Hao** constructed the model, designed the controller and wrote the manuscript in the study. Ms. **MA Songjing** contributed to the figures, tables and experimental analysis of the paper. Dr. **HUA Bing** participated in the research design and discussions. Dr. **LU Zhenkun** supervised the research, reviewed the results, and

contributed to manuscript revision. Prof. **WU Yunhua** analyzed the data, result interpretation and manuscript revision. All authors provided feedback on the manuscript draft and approved the submission.

**Competing interests** The authors declare no competing inrests.

(Production Editor: WANG Jie)

# 基于干扰观测器的组合体航天器预设时间姿态控制

张 浩[1], 马松靖[1], 华 冰[1], 逯振坤[2], 吴云华[1]

(1.南京航空航天大学航天学院,南京 211100,中国;2.温州理工学院机器人工程学院,温州 325000,中国)

**摘要:**空间在轨服务任务中,服务航天器通常需要与目标航天器对接形成组合体航天器执行后续任务,且两者之间的协同姿态控制是一个具有挑战性的技术。针对组合体航天器姿态控制过程中存在转动惯量不确定性、通信时延和外界干扰等问题,提出了一种具有预设时间收敛的鲁棒协同控制方法。首先,建立组合体航天器分布式控制模型,并设计一种可以直接设置收敛时间的预设性能函数对系统的瞬态和稳态性能进行描述。然后,结合反步法设计基于预设时间性能的姿态控制器来实现组合体航天器快速准确地姿态机动。进一步,先引入干扰观测器用于估计转动惯量不确定性和外部扰动组成的复合扰动来提升控制器的鲁棒性;同时基于一致性理论,设计姿态协同控制项来补偿通信时延导致的控制力矩不同步的影响。接着利用李雅普诺夫函数证明系统的稳定性。最后,通过数学仿真验证所提控制器能够在上述外界干扰下实现组合体航天器在预设时间内准确地姿态协同控制。

**关键词:**组合体航天器;姿态机动;预设时间控制;干扰观测器;鲁棒协同控制

**研究亮点:**

1. 面向姿态控制收敛时间难以直接设定的问题,设计可直接预设收敛时间的性能函数,并引入可穿越误差转换函数,实现姿态误差的无约束转换;

2. 针对组合体航天器转动惯量不确定性与外部扰动等耦合影响,引入干扰观测器对复合扰动进行在线估计与补偿,提高姿态控制的鲁棒性;

3. 针对组合体航天器存在通信时延导致的姿态信息不同步问题,基于一致性理论设计姿态协同控制项,实现组合体航天器的高精度姿态协同控制。